Available online at www.sciencedirect.com
SCIENCE DIRECT®
PERGAMON
Engineering Fracture Mechanics 70 (2003) 2187–2197
Engineering Fracture Mechanics
www.elsevier.com/locate/engfracmech

Fatigue crack growth behavior of Sn–Pb and Sn-based lead-free solders

Jie Zhao [a,b,*], Yoshiharu Mutoh [b], Yukio Miyashita [b], Lai Wang [a]

[a] *Department of Materials Engineering, Dalian University of Technology, Dalian city, Liaoning Province 116023, PR China*
[b] *Nagaoka University of Technology, Nagaoka 940-2188, Japan*

Received 31 December 2001; received in revised form 15 August 2002; accepted 4 October 2002

Abstract

Solder alloys of lead-rich composition have been commonly used as joining materials in electronic package. However, because of environmental concerns, lead-free solders will replace lead-rich solders more and more in the future. The fatigue characteristics of the solders used are most important in assessing the reliability of joints in electronic packaging. In the present study, the fatigue crack growth (FCG) behavior of a wide variety of solders of both lead-rich and lead-free types has been investigated under a range of mean stresses and frequencies. Both time dependent and time independent (cyclic dependent) behaviors were observed. In the cyclic dependent crack growth regime, the FCG rates could be expressed as a function of either ΔK_{eff} or ΔJ. Further, the lead-free solders were found to have a higher resistance to FCG than did the lead-rich solders. In the time dependent crack growth regime, the FCG rates were found to be a function of C^*. The point of transition between time dependent and time independent behavior was found to depend on the homologous temperature and strength of the alloys.

Keywords: Solder; Fatigue crack growth; Cyclic dependence; Time dependence; Creep effect

1. Introduction

There has been much research into soldering technology in recent years because of increase interest in the reliability of solder joints in electronic packaging. In addition environmental concerns have led to the introduction of lead-free solders to replace the traditional lead-rich solders. In both of these areas, the low-cycle fatigue properties of solders are important considerations. The cyclic loads arise largely because of restraints against thermal expansion during temperature fluctuations as well as from differences in the thermal expansion coefficients of the components [1]. Since a large part of the low-cycle fatigue lifetime is spent in crack propagation, a knowledge of the factors affecting the rate of fatigue crack propagation is therefore useful in assessing the life of solder joints [1–3]. Much low-cycle fatigue research has already been

* Corresponding author. Address: Department of Materials Engineering, Dalian University of Technology, Dalian city, Liaoning Province 116023, PR China. Tel.: +86-411-470-7636; fax: +86-411-470-8116.
E-mail address: jiezhao@dlut.edu.cn (J. Zhao).

0013-7944/03/$ - see front matter © 2002 Elsevier Ltd. All rights reserved.
doi:10.1016/S0013-7944(02)00252-7

done using smooth specimens, which in one case involved the indirect determination of the crack length [4,5]. However, only a few studies have involved the use of the standard ASTM pre-cracked specimens [6–8]. In one such study [6], Logsdon et al. found that the rate of fatigue crack growth (FCG) in a Pb–Sn solder could be expressed as a function of ΔK. It was also observed that the fatigue cracks grew in a transgranular mode, cutting through both tin rich and lead-rich regions.

As homologous temperature of solders is quite high, creep deformation can play a role during normal operations. The role of creep has been studied by Vaynman et al. [9] who determined the effect of strain range, frequency and hold time on the isothermal fatigue behavior of smooth specimens of 96.5Pb–3.5Sn solder. They found that at frequencies below 10^{-2} Hz the cyclic lifetimes were reduced. Tensile hold times were found to also reduce the fatigue lifetimes. In studies of the isothermal fatigue behavior of eutectic solders, it was found that there were critical frequencies (3×10^{-4} Hz at 35 °C [10] and 3×10^{-3} Hz at 150 °C [11]). Other recent investigations of Sn–Pb solders [7,8] have also indicated a change in FCG behavior from time independent (cyclic dependent) to time dependent growth with increase in stress ratio (mean stress) or decrease in cyclic frequency. Despite the research already been carried out, it is clear the much more needs to be done, particularly for lead-free solders.

The aim of the present work was to compare the FCG behavior of traditional Sn–Pb and Sn–Ag solders with that of more recently developed Sn–Ag–Cu and Sn–Ag–Cu–Bi solders. The time dependency of the FCG process was investigated by either increasing the mean load or decreasing the cyclic frequency. Creep crack growth (CCG) tests were also carried out for comparison.

2. Experimental procedures

The materials used were six as-cast solders, which were Sn–Pb type solders and Sn–Ag type solders as shown in Table 1. Young's modulus, liquidus and solidus of the solders are also listed in the table.

FCG and CCG tests were conducted in air at a constant temperature of 20 °C and a constant relative humidity of 55%. The specimens were of the CT type with the following dimensions: width (W) 39 mm, height (H) 50 mm, and thickness (B) 4 mm for the 63Sn–37Pb and 6 mm for other solders. The tests were performed in a servo-hydraulic fatigue-testing machine in accord with ASTM standard test method E647-95a. The crack length, a, was measured with a traveling microscope with precision of 10 μm, and the sensitivity of the applied cyclic loads was known to be 0.2 N. The FCG tests were conducted at testing conditions listed in Table 2. The side surfaces of all the specimens were hand-polished before test to facilitate the measurement of crack lengths and the observation of crack paths.

Due to the low yield strength of the alloys, large plastic zones might form at the crack tips during FCG. Therefore, the FCG rates were correlated by using ΔJ, a parameter for large scale yielding conditions. ΔK, a parameter for small scale yielding conditions can still be used for high temperature fatigue crack propagation if the zone of inelastic deformation at the crack tip is small in size compared to crack length and the

Table 1
The solders used in current tests

Material	Sn (wt.%)	Pb (wt.%)	Ag (wt.%)	Cu (wt.%)	Bi (wt.%)	Liquidus (°C)	Solidus (°C)	Young's modulus E (GPa)
95Pb–5Sn	5	95	–	–	–	312	270	20
63Sn–37Pb	63	37	–	–	–	183	183	30
Sn–3.5Ag	96.5	–	3.5	–	–	221	221	51
SnAgCu	96.5	–	3	0.5	–	219	217	54
SnAgCuBi1	95.5	–	3	0.5	1	219.5	213	52
SnAgCuBi3	93.5	–	3	0.5	3	219.5	207	53

Table 2
The testing conditions for the solders used

Material	Frequency (Hz)	Stress ratio (R)			
		0.1	0.3	0.5	0.7
95Pb–5Sn	10	○	○	○	○
	1	○	–	–	–
	0.1	○	–	–	–
	0.01	○	–	–	–
63Sn–37Pb	10	○	○	○	○
	1	○	–	–	–
	0.1	○	–	–	–
Sn–3.5Ag	10	○	○	○	○
	1	○	–	–	–
	0.1	○	–	–	–
SnAgCuBi3	10	○	–	○	○
	0.1	○	–	–	–
SnAgCuBi1	10	○	–	○	○
SnAgCu	10	○	–	–	○

size of the uncracked ligament [12], was also used to plot the data for comparison. The ΔJ-value was calculated according to the following equation [13]:

$$\Delta J = \frac{2A(1+\alpha)}{Bb(1+\alpha^2)} \tag{1}$$

where A is the area under the load vs load-line displacement curve, $b = W - a$. B, W and a are the thickness, the width and the crack length, respectively, and

$$\alpha = \sqrt{\left(\frac{2a}{b}\right)^2 + 2\left(\frac{2a}{b}\right) + 2} - 2\frac{a}{b} - 1 \tag{2}$$

The load-line displacement was measured by means of a clip gage mounted at the crack mouth. The ΔK-value was calculated according to the equation in the ASTM E647-95a standard.

Because of the high homologous temperature of the solders, C^*, which is regarded as a crack tip parameter, which characterizes the CCG rate at elevated temperatures in ductile materials [14,15] was used to discuss the time dependent FCG behavior. The C^*-value was estimated by using the following equation [16]:

$$C^* = \frac{P\dot{V}_c}{BW}\left[\frac{n}{n+1}\left(\frac{2}{1-a/W} + 0.522\right)\right] \tag{3}$$

where P is the applied load, $\dot{V}_c$ is the load-line displacement rate. For cyclic loading, P is the maximum applied load, $\dot{V}_c$ is the rate of upper load-line displacement. n is the creep exponent which has a weak dependency on the value of C^* for CT specimen. The values of n were 8 for 95Pb–5Sn [17], 5.9 for 63Sn–37Pb [18], 6.05 for other solders [19] as it was reported that Sn–Ag and Sn–Ag–X (X = Bi or Cu) solders have comparable values of creep exponent [20].

3. Experimental results and discussions

3.1. Fatigue crack growth behavior

It is known that crack closure plays an important role in FCG behavior [21]. In the present study, an attempt to measure a crack closure point from a down load curve during cyclic loading was made using both strain gauges attached on the back faces and a clip gage at the crack mouth. Obvious crack closure level were only detected in a SnAgCuBi1 specimen tested at $R = 0.1$, as shown in Fig. 1. The value of the stress intensity factor at the crack closure point on the unloading curve was about 0.86 MPa $m^{1/2}$.

Generally, a FCG process can be described either by cyclic dominance or by time dominance under a certain testing condition. A cyclic dependent behavior is dominant for the tests at low stress ratios, high frequencies or low homologous temperature, while a time dependent behavior becomes dominant when creep effect becomes dominant. Fig. 2 shows the FCG rates as a function of ΔJ for the specimens tested

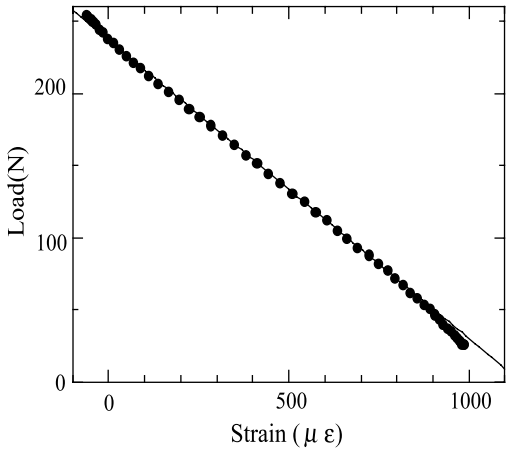

(a) Load-strain curve(down load) measured from the back surface

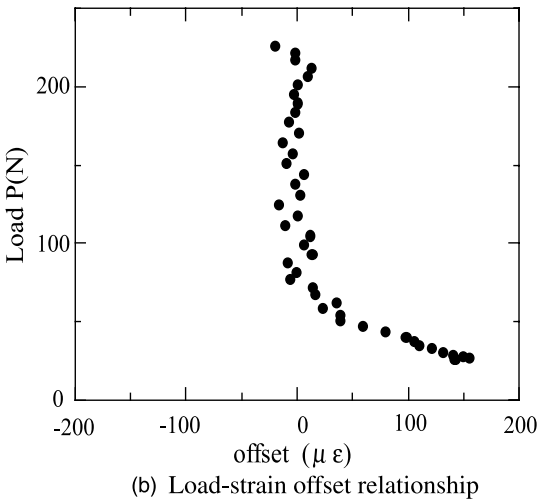

(b) Load-strain offset relationship

Fig. 1. Crack closure in the Sn–3Ag–0.5Cu–1Bi solder test under $R = 0.1$ and $f = 10$ Hz (at $\Delta K = 2.7$ MPa $m^{1/2}$).

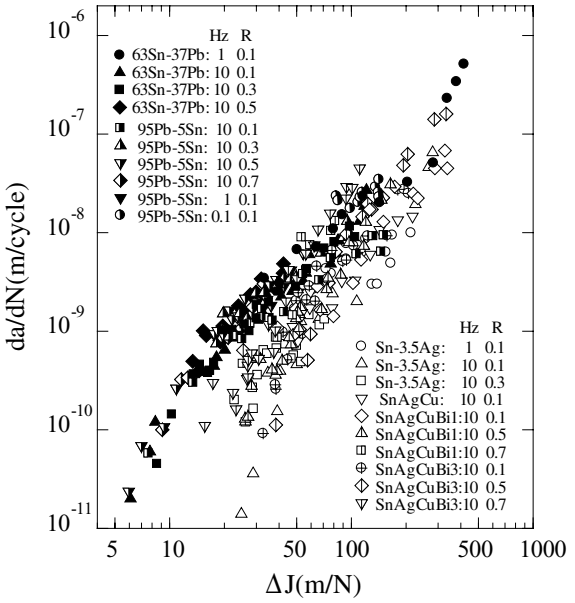

Fig. 2. Relationship between ΔJ and $\mathrm{d}a/\mathrm{d}N$ for the current solders tested under cyclic dependent condition.

under cyclic dependent conditions. It is found that the Sn–Pb and Sn-based lead-free type solders can be plotted into two data bands. The Sn–Pb solders exhibit systematically higher FCG rates than the Sn-based lead-free solders. The difference is large at the low ΔJ region, while it becomes small with increasing value of ΔJ. The linear relationships between logarithmic $\mathrm{d}a/\mathrm{d}N$ and ΔJ for the Sn–Pb and Sn-based lead-free solders except for the low crack growth rate regions can be expressed as

$$\mathrm{d}a/\mathrm{d}N = 3.8 \times 10^{-12}\Delta J^{1.9} \quad \text{for Sn–Pb solders} \tag{4}$$

$$\mathrm{d}a/\mathrm{d}N = 2.6 \times 10^{-13}\Delta J^{2.1} \quad \text{for Sn-based lead-free solders} \tag{5}$$

For the purpose of comparison, the results were also plotted in terms of ΔK_{eff} (where $\Delta K_{\mathrm{eff}} = K_{\max} - \max(K_{\min}, K_{\mathrm{cl}})$) as shown in Fig. 3, where the testing conditions were the same as those in Fig. 2. In Fig. 3, it is seen that the results fall into three material-sensitive bands. After normalizing the effective stress intensity factor range ΔK_{eff} by using Young's modulus E of the solders (see Table 1), all the data fall in a data band regardless of materials and testing conditions as shown in Fig. 4. The expression relating $\mathrm{d}a/\mathrm{d}N$ and $\Delta K_{\mathrm{eff}}/E$ is

$$\mathrm{d}a/\mathrm{d}N = 6.83 \times 10^{-12}(\Delta K_{\mathrm{eff}}/E)^{4.05} \tag{6}$$

It is known that under small scale yielding condition, the relationship between ΔK and ΔJ (the symbol of ΔJ_{cal} is employed in order to distinguish from the experimental ΔJ) can be expressed as [22]

$$\Delta J_{\mathrm{cal}} = \frac{\Delta K_{\mathrm{I}}^2}{E} \tag{7}$$

where E is the Young's modulus. After calculating the values of ΔJ_{cal} based on the data in Fig. 3, the relationship between $\mathrm{d}a/\mathrm{d}N$ and calculated ΔJ_{cal} is shown in Fig. 5. In the figure, the experimental curves of Sn–Pb and Pb-free solders are also plotted. Although scattering of data existed, agreement can be observed

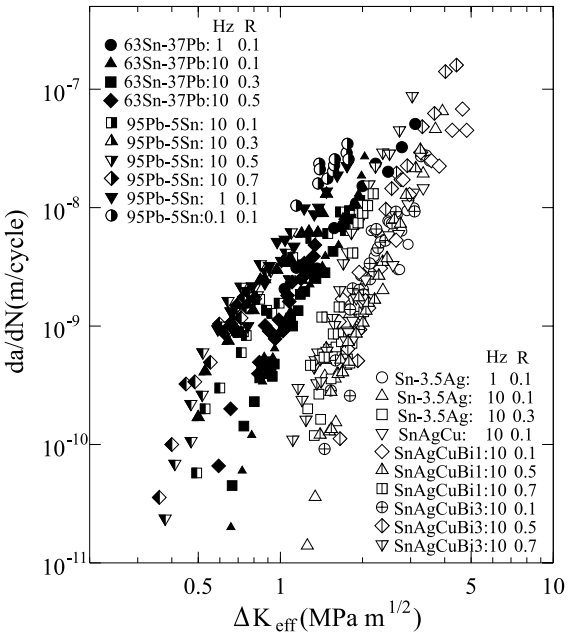

Fig. 3. Relationship between ΔK_{eff} and $\mathrm{d}a/\mathrm{d}N$ for the current solders tested under cyclic dependent condition.

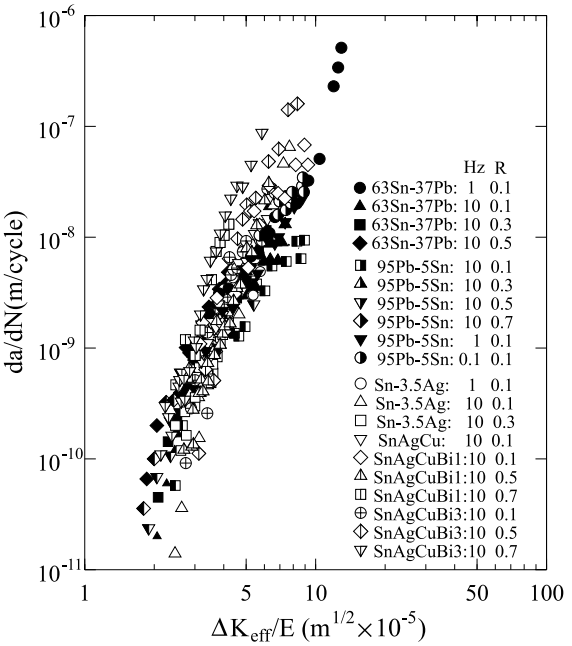

Fig. 4. The $\Delta K_{\text{eff}}/E$–$\mathrm{d}a/\mathrm{d}N$ relationship in the Sn–Pb and Sn-based lead-free solders.

between the calculated values and the experimental results. It implies that there was not much overall plastic deformation involved in cyclic dependent tests.

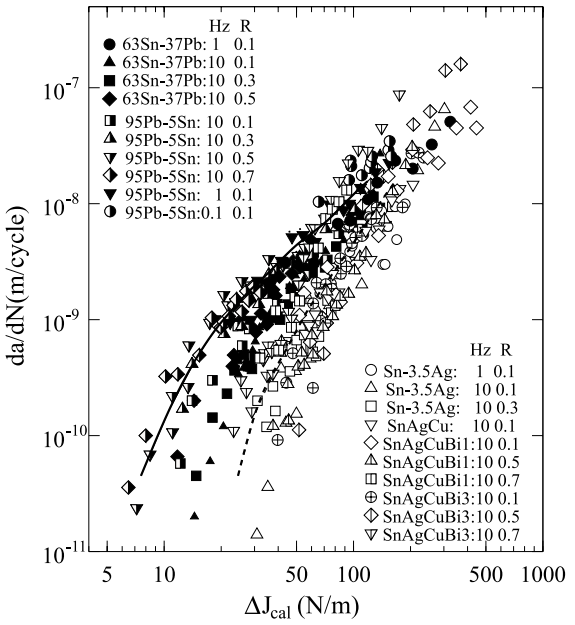

Fig. 5. Relationship between calculated ΔJ_{cal} and da/dN. The solid and dotted lines represent the experimental results of the Sn–Pb and Sn-based lead-free solders tested under cyclic dependent condition, respectively.

3.2. Near-threshold behavior

The threshold level for FCG is an important characteristic to be considered in assessing the resistance of a material to FCG. It has been demonstrated that the FCG rates at low stress intensities are sensitive to microstructure, load ratio and environment, while the effective threshold stress intensity range is intrinsically insensitive to these factors [6]. Although the threshold values at a da/dN of 10^{-11} m/cycle of the solders were not measured, it is still clear from the near-threshold data in Figs. 2 and 3 that the Sn-based lead-free solders have higher threshold values than Sn–Pb solders. The values of ΔK_{th}, $\Delta K_{th,eff}$ and ΔJ_{th} at a da/dN of 10^{-11} m/cycle (for the specimens tested at $R = 0.1$) were extrapolated based on the last 4 data points and are listed in Table 3. The values of ΔK_{th} were almost the same as those of $\Delta K_{th,eff}$ because of negligible crack closure level. The level of $\Delta K_{th,eff}$ for the 95Pb–5Sn solder is the lowest among all the solders. The Sn–3.5Ag solder showed higher threshold values than those for 95Pb–5Sn and 63Sn–37Pb solders, which seems to reflect the strengthening role of Ag_3Sn intermetallics.

3.3. Time dependent fatigue crack growth behavior

For the data tested at high stress ratios and low frequencies, different da/dN–ΔJ behavior from the former results was observed as shown in Fig. 6. The data shift to the left with a random distribution with

Table 3
The extrapolated threshold values of the solders tested at 10 Hz and $R = 0.1$

Material	ΔK_{th} (MPa m$^{1/2}$)	ΔK_{theff} (MPa m$^{1/2}$)	$\Delta K_{effth}/E$ (m$^{1/2}$ × 10^{-5})	$\Delta J_{th}(\Delta J_{effth})$ (N/m)
95Pb–5Sn	0.47	0.40	2.00	5.2
63Sn–37Pb	0.65	0.65	2.17	5.3
Sn–3.5Ag	1.2	1.2	2.35	23

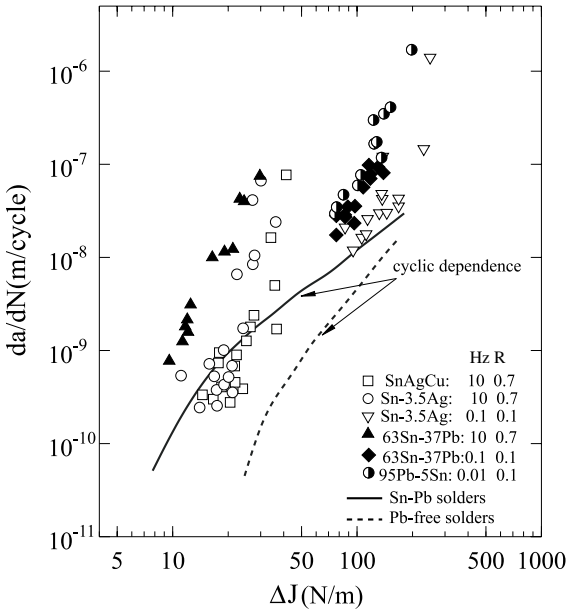

Fig. 6. Relationship between ΔJ and da/dN for the current solders tested under high stress ratios and low frequencies, the solid and dotted lines represent the results of the Sn–Pb and Sn-based lead-free solders tested under cyclic dependent condition, respectively.

increasing stress ratio and decreasing frequency. Similar behavior was also observed at da/dN–K_{eff} relationship. Because of the low homologous temperatures of current solders, the significant increase of crack growth rates was attributed to increasing influence of creep deformation during crack propagation. Therefore, it is supposed that although either ΔJ or ΔK_{eff} can be used to relate the FCG behavior under cyclic dependent condition, they are not suitable for describing the FCG behavior where extensive creep deformation occurs.

In the region of time dependent crack growth, fracture mechanics parameters, such as $K_{\max}$ and J, are not valid, whereas the modified J-integral or C^* is the effective parameter. By using the same results as those in Fig. 6, the da/dt–C^* relationship for the specimens tested at high stress ratios and low frequencies is shown in Fig. 7, together with the data of CCG tests. It is found that all the data under cyclic load could be plotted in a data band, in accord with the CCG results. It is therefore supposed that the FCG process is dominantly a time dependent process for the current solders under the testing conditions listed in Fig. 7. The expression between da/dt and C^* is

$$da/dt = 8.34 \times 10^{-8} C^{*1.08} \tag{8}$$

Generally, C^* is used to describe creep crack propagation under static load, while the current work firstly made use of C^* to correlate the time dependent cyclic crack propagation. Although good experimental agreement was observed between time dependent cyclic data and static data in the present research and it seems that C^* may be valid to correlate time dependent cyclic crack growth, further experiments and theoretical work are needed to substantiate it.

After further analyzing the results in Figs. 2, 3 and 7 it can be seen that the 95Pb–5Sn solder only exhibited time dependent FCG behavior at frequency as low as 0.01 Hz. Further, the Sn–Ag–Cu–Bi solders did not show time dependent FCG behavior under current testing conditions. It appears that these solders have a higher resistance to the transition from cyclic dependent to time dependent behavior. It is assumed that the higher resistance of the 95Pb–5Sn solder may attributed to the lower homologous temperature,

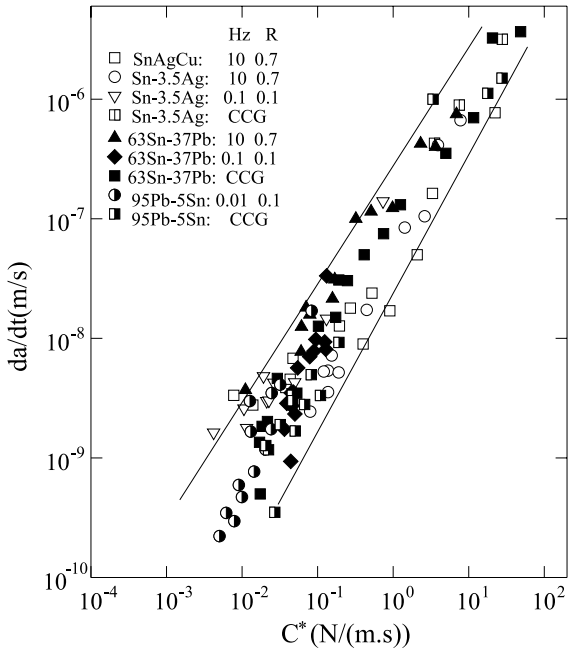

Fig. 7. The C^*–da/dt relationship in the Sn–Pb and Sn-based lead-free solders tested under high stress ratios and low frequencies, together with the data of CCG.

while the higher resistance of the Sn–Ag–Cu–Bi solders might result from the solid solution hardening effect of Bi content as well as the strengthening effect of intermetallics Cu_6Sn_5 and Ag_3Sn.

3.4. Fatigue crack growth processes

From the foregoing results and observation, FCG processes of the present solders are schematically summarized in Fig. 8. At a low stress ratio and high frequency, the FCG behavior is dominantly cyclic dependent, cracks propagates predominantly in a transgranular manner [23], and either ΔJ or ΔK_{eff} can be used to relate the crack growth rates. At high stress ratio and low frequency, the FCG behavior is

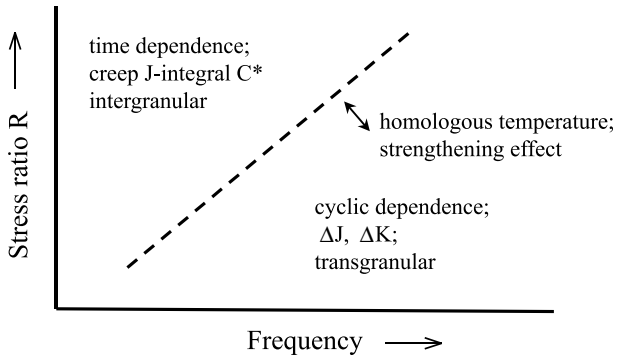

Fig. 8. Schematics of FCG processes in the solders.

dominantly time dependent, intergranular fracture becomes dominant [23], and C^* can be used to describe the crack growth rates. The strengthening effect and the change of homologous temperature shift the transition condition between cyclic dependent process and time dependent process. The increase of homologous temperature shifts the transition condition to the left in Fig. 8 and enlarges the time dependent region, while strengthening effect of materials extends the cyclic dependent region and moves the transition condition to the right in Fig. 8.

4. Conclusions

Based on the foregoing results and discussion for six solders of 95Pb–5Sn, 63Sn–37Pb, Sn–3.5Ag, Sn–3Ag–0.5Cu, Sn–3Ag–0.5Cu–1Bi and Sn–3Ag–0.5Cu–3Bi, the main conclusions are summarized as follows:

1. The FCG behavior of all the Sn–Pb and Sn-based lead-free solders can be described either by cyclic dominance or by time dominance under current testing conditions. A cyclic dependent behavior was dominant for tests at low stress ratios and high frequencies, while a time dependent behavior became dominant at high stress ratios and low frequencies. The latter effect was attributed to increasing creep with increasing stress ratio and decreasing frequency.
2. Obvious crack closure levels were only detected in the Sn–3Ag–0.5Cu–1Bi solder where the value of K_{cl} was about 0.86 MPa $m^{1/2}$. The FCG rates could be expressed as a function of either ΔJ or ΔK_{eff} under cyclic dependent testing conditions. In da/dN–ΔJ relationship, the Sn–Pb solders exhibited systematically higher FCG rates than the Sn-based lead-free solders. After normalizing the effective stress intensity factor range ΔK_{eff} by using Young's modulus E of the solders, all the data fall in a data band regardless of materials and testing conditions, which can be expressed as: $da/dN = 6.83 \times 10^{-12}(\Delta K_{eff}/E)^{4.05}$.
3. For the experiments under time dependent testing conditions, the crack growth rates were found to be a function of C^* and the results were in accord with the CCG data. The expression between da/dt and C^* is: $da/dt = 8.34 \times 10^{-8} C^{*1.08}$.

Acknowledgements

The authors greatly thank Mr. T. Ori, Oki Electric Industry Co., Ltd. for supplying the materials.

References

[1] Guo Z, Conrad H. Fatigue crack growth rate in 63Sn37Pb solder joints. J Electron Packaging 1993;115(6):159–64.
[2] Solomon HD. Life prediction and accelerated testing. In: Frear DR et al., editors. The Mechanics of Solder Alloy Interconnects. New York: Van Nostrand Reinhold; 1994. p. 199–313.
[3] Kariya Y, Otsuka M. Mechanical fatigue characteristics of Sn–3.5Ag–X solder alloys. J Electron Mater 1998;27:1229–35.
[4] Liu PL, Shang JK. Influence of microstructure on fatigue crack growth behavior of Sn–Ag solder interfaces. J Electron Mater 2000;29(5):622–7.
[5] Pao YH, Govila R, Badgley S. Thermal fatigue fracture of 90Pb/10Sn solder joints. In: Chen WT, Abe H, editors. Proc Advances in Electronic Packaging. ASME/JSME, EEP, vol. 1-1, 1992. p. 291–300.
[6] Logsdon WA, Liaw PK, Burke MA. Fracture behavior of 63Sn–37Pb solder. Engng Fract Mech 1990;36(2):183–218.
[7] Zhao J, Miyashita Y, Mutoh Y. Fatigue crack growth behavior of 95Pb–5Sn solder at various stress ratios and frequencies. Int J Fatigue 2000;22:665–73.
[8] Zhao J, Mutoh Y, Miyashita Y, Ogawa T, McEvily AJ. Fatigue crack growth behavior in 63Sn–37Pb and 95Pb–5Sn solder materials. J Electron Mater 2001;30(4):415–21.
[9] Vaynman S, Fine ME, Jeannotte DA. Isothermal fatigue of low tin lead based solder. Metall Trans A 1988;19A(4):1051–9.

[10] Solomon HD. Electronic packaging: materials and processes. Sortell JA, editor, OH: Metals Park, ASM, 1985. p. 29.
[11] Solomon HD. Low-frequency, high-temperature low-cycle fatigue of 60Sn/40Pb solder. In: Solomon HD et al., editors. Low Cycle Fatigue. ASTM STP942. Philadelphia, 1988. p. 342–369.
[12] Suresh S. Fatigue of materials. 2nd ed. New York: Cambridge University Press; 1998. p. 598.
[13] Clarke GA, Landes JD. Evaluation of the *J* integral for the compact specimen. J Test Eval, JTEVA 1979;7(5):264–9.
[14] Landes JD, Begley JA. A fracture mechanics approach to creep crack growth. In: Mechanics of Crack Growth. ASTM STP 590. Philadelphia, 1976. p. 128–148.
[15] Nikbin KM, Webster GA, Turner CE. Relevance of nonlinear fracture mechanics to creep cracking. In: Crack and Fracture. ASTM STP 601. Philadelphia, 1976. p. 47–62.
[16] Saxena A. Creep crack growth in high temperature ductile materials. Engng Fract Mech 1991;40(4/5):721–36.
[17] Frost HJ, Ashby ME. Deformation-mechanism maps—the plasticity and creep of metals and ceramics. Oxford: Pergamon Press, UK; 1982. p. 28–29.
[18] Vaynman S, Ghosh G, Fine ME. Effects of palladium and solder aging on mechanical and fatigue properties of tin–lead eutectic solder. J Electron Mater 1998;27(11):1223–8.
[19] Hua F, Glazer J. Lead-free solders for electronic assembly. In: Mahidhara RK, Frear DR, Sastry SML, Murty KL, Liaw PK, Winterbottom W, editors. Design and Reliability of Solder Interconnections. The Minerals, Metals and Materials Society, 1997. p. 65–73.
[20] Frear DR. The mechanical behavior of interconnect materials for electronic packaging. JOM 1996;48:49–53.
[21] Liaw PK. Overview of crack closure at near-threshold fatigue crack growth levels. In: Newman Jr JC, Elber W, editors. Mechanics of Fatigue Crack Closure, ASTM STP 982, ASTM. Philadelphia, 1988. p. 62–92.
[22] Anderson TL. Fracture mechanics. 2nd ed. Florida: CRC Press; 1995. p. 563.
[23] Zhao J. Fatigue crack growth behavior of solders, doctor thesis, Nagaoka University of Technology, 2001.